

ON THE PARTITIONING OF ENERGY IN LOVE WAVE DIFFRACTION  
PROBLEMS IN Laterally DISCONTINUOUS STRUCTURES

M.H. Kazi<sup>I</sup> AND A. Niazy<sup>II</sup>

SUMMARY

We investigate partitioning of energy in two-dimensional diffraction problems of propagation of plane harmonic Love waves incident normally upon the plane of discontinuity in laterally discontinuous structures (involving surface-steps or impedance contrasts) with finite or infinite substrata. We show that for the finite substratum problems the total incident energy is exactly partitioned into the total reflected and transmitted energies concentrated in normal modes, whereas in the corresponding half-space problems the total incident energy is greater than the sum of the energies reflected and transmitted in normal modes. The implications of this result are discussed with particular reference to earthquake engineering.

TRANSMISSION MATRICES FOR PLANE-WAVE AND VARIATIONAL APPROXIMATIONS

In a series of papers (Kazi (1978a,b), Kazi (1979), Niazy and Kazi (1980a,b)) we applied a method based upon spectral representation of the Love wave operator alongwith Schwinger-Levine variational principle to investigate the two-dimensional problems of diffraction of plane harmonic Love waves, incident normally upon the plane of discontinuity in each of the following laterally discontinuous structures:

1. An infinite strip with a surface step (Fig.1) (Kazi (1979)).
2. Welded layered half-strips of equal overall thickness (Fig.2) (Niazy and Kazi (1980b)).
3. A half-space with a surface step (Fig.3) (Kazi (1978a,b)).
4. Welded layered quarter-spaces with a plane surface (Fig.4) (Niazy and Kazi (1980a)).

Diffraction of Love waves is described by means of a scattering matrix and approximate expressions for its elements are sought through the plane wave and variational approximations. Complex reflection and transmission co-efficients are then obtained through a transmission matrix related to the scattering matrix.

The displacement fields in domains I ( $x < 0$ ) and II ( $x > 0$ ) in all the four structures are denoted by  $\exp(-i\omega t)v(x,z)$  and  $\exp(-i\omega t)v'(x,z)$  respectively,  $\omega$  being the angular frequency, so that the wave motion is entirely SH in character. For an infinite strip with a surface step (Fig.1)

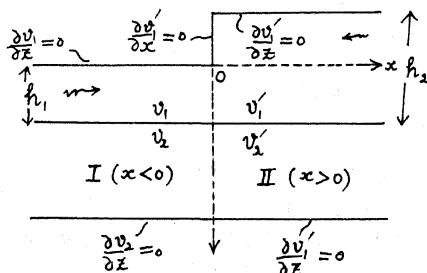


Fig.1. The geometry of the problem of the propagation of Love waves normally incident upon the vertical plane of discontinuity ( $x=0$ ) in a 2-layer model consisting of an infinite strip with a surface step.

I Department of Mathematical Sciences, University of Petroleum and Minerals, Dhahran, Saudi Arabia

II Department of Earth Sciences, University of Petroleum and Minerals, Dhahran, Saudi Arabia.

Fig.2. The geometry of the problem of Love wave propagation in welded layered half-strips. The Love waves are normally incident on the plane of contact  $x=0$ .

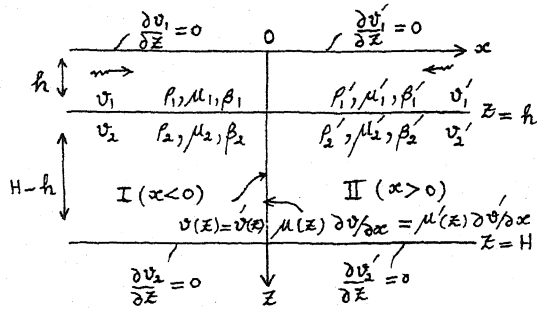


Fig.3. The geometry of a surface step over a half-space. Love waves are normally incident on the vertical plane of discontinuity.

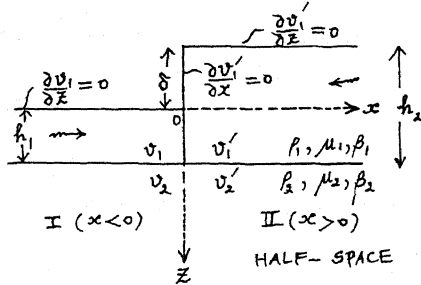
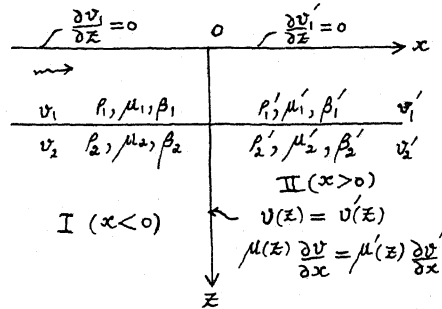


Fig.4. The geometry of welded layered quarter spaces. Love waves are incident normally upon the vertical plane ( $x=0$ ) of welded contact.



$v(x, z)$  and  $v'(x, z)$  are given by (see Kazi (1979))

$$\begin{aligned}
 v(x, z) = & - \left( \sum_{m=1}^r \{A_m \exp(-ik_m |x|) + B_m \exp(ik_m |x|)\} \chi_m(z) \right) \\
 & + \sum_{j=1}^m C(k_j) \exp(-k_j |x|) \psi(z, k_j), \quad x < 0 \\
 v'(x, z) = & \sum_{m=1}^s \{A'_m \exp(-ik'_m x) + B'_m \exp(ik'_m x)\} \chi'_m(z) \\
 & + \sum_{j=1}^{\infty} C'(k'_j) \exp(-k'_j x) \psi'(z, k'_j), \quad x > 0
 \end{aligned} \quad (1)$$

where  $\lambda_m = k_m^2$ ,  $k_m > 0$ ,  $m = 1, 2, \dots, r$ , are  $r$  positive real eigenvalues satisfying the dispersion equations

$$\mu_1 \sigma_1 \tanh \sigma_1 h_1 - \mu_2 \sigma_2 \tanh \sigma_2 (H - h_1) = 0 \quad (2)$$

$$\sigma_1 = (\omega^2 / \beta_1^2 - \lambda)^{1/2}, \quad \sigma_2(\lambda) = (\lambda - \omega^2 / \beta_2^2)^{1/2}, \quad (3)$$

and  $\lambda_j = (ik_j)^2$ ,  $k_j$  being real and positive, are negative real roots of equation (2).  $\chi_m(z)$ ,  $m=1,2,\dots,r$ , and  $\psi(z,k)$  are normalized eigenfunctions corresponding to the positive and negative real/eigen-values respectively. These functions form an orthonormal set. The primed quantities in the expression for  $v'(x,z)$  are similarly defined for domain II. For welded layered half-strips of equal overall thickness (Fig.2) we have the same expressions for  $v$  and  $v'$  as in (1) but with different formulae for eigenfunctions.

For the problem of a half-space with a surface step (Fig.3), we have (see Kazi (1978a)) in

DOMAIN I ( $x < 0$ ,  $z \geq 0$ )

$$v(x,z) = -\left\{ \sum_{m=1}^r A_m \exp(-ik_m |x|) + B_m \exp(ik_m |x|) \right\} \chi_m(z) + \int_0^{\omega/\beta_2} [C(k) \exp(-ik|x|) + D(k) \exp(ik|x|)] \phi(z,k) dk + \int_0^{\infty} E(k) \exp(-k|x|) \psi(z,k) dk \quad (4)$$

and in DOMAIN II ( $x > 0$ ,  $z \geq -\delta = h_1 - h_2$ )

$$v'(x,z) = \left\{ \sum_{m=1}^s [A'_m \exp(-ik'_m x) + B'_m \exp(ik'_m x)] \chi'_m(z) + \int_0^{\omega/\beta_2} [C'(k') \exp(-ik'x) + D'(k') \exp(ik'x)] \phi'(z,k') dk' + \int_0^{\infty} E'(k') \exp(-k'x) \psi'(z,k') dk' \right\} \quad (5)$$

where  $\chi_m$  are eigenfunctions corresponding to solutions  $\lambda = \lambda_m = k_m^2$ ,  $m=1,2,\dots,r$  of the Love wave dispersion equation

$$\mu_1 \sigma_1 \tan \sigma_1 h_1 - \mu_2 \sigma_2 = 0, \quad \sigma_1(\lambda) = \left( \frac{\omega^2}{\beta_1^2} - \lambda \right)^{1/2}, \quad \sigma_2(\lambda) = \left( \lambda - \frac{\omega^2}{\beta_2^2} \right)^{1/2}; \quad (6)$$

$\psi(z,k)$  are the improper eigenfunctions in the domain,  $x < 0$ , corresponding to the continuum of improper eigenvalues  $\lambda = (ik)^2$ ,  $k > 0$  and representing non-propagated modes. The improper functions  $\phi(z,k)$  corresponding to the eigenvalues in the range  $(0, \omega^2/\beta_2^2)$  have expressions similar to those for  $\psi(z,k)$  except for the fact that  $\lambda = k^2$  and  $0 < k \leq \omega/\beta_2$ . These correspond to waves travelling in the  $x$ -direction. The primed quantities in (5) can similarly be defined. For welded layered quarter-spaces (Fig.4) we have the same expression for  $v(x,z)$  and  $v'(x,z)$  as in Eqs. (4) and (5) but with different formulae for  $\chi_m(z)$ ,  $\phi(z,k)$  and  $\psi(z,k)$

etc. The functions  $\chi_m(z)$ ,  $\phi(z,k)$  and  $\psi(z,k)$  form an orthonormal set. When  $r=1$ ,  $s>1$  (i.e. there is a single (fundamental) mode in the left-hand domain and there are  $s$  modes on the right) the transmission matrix  $T^P$  for the plane-wave approximation in all the four problems mentioned above has the form (see for example Kazi (1979))

$$\underline{T}_p = \frac{1}{N} \begin{bmatrix} -2+N & -2\lambda_{11}P_{11} & -2\lambda_{21}P_{21} & \dots & -2\lambda_{s1}P_{s1} \\ -2P_{11}/\lambda_{11} & -2P_{11}^2+N & -2P_{11}\lambda_{21}P_{21}/\lambda_{11} & \dots & -2P_{11}\lambda_{s1}P_{s1}/\lambda_{11} \\ -2P_{21}/\lambda_{21} & -2P_{21}P_{11}\lambda_{11}/\lambda_{21} & -2P_{21}^2+N & \dots & -2P_{21}\lambda_{s1}P_{s1}/\lambda_{21} \\ \vdots & \vdots & \vdots & \ddots & \vdots \\ -2P_{s1}/\lambda_{s1} & -2P_{s1}P_{11}\lambda_{11}/\lambda_{s1} & \dots & \dots & -2P_{s1}^2+N \end{bmatrix} \quad (7)$$

where  $N = 1 + P_{11}^2 + P_{21}^2 + \dots + P_{s1}^2$ ,  $\lambda_{im} = (k'_i/k_m)^{1/2}$ ,  $(8)$

and the coupling co-efficients are given by the integrals

$$\lambda_{im}P_{im} = \int_0^H \mu(n)\chi'_i(n)\chi_m(n)dn, \quad \begin{matrix} i = 1, 2, \dots, s, \\ m = 1, 2, \dots, r \end{matrix} \quad (9)$$

for the finite substratum problems.  $H$  is replaced by  $\infty$  in (8) for the half-space problems. Similarly for the same case ( $r=1, s \geq 1$ ) the transmission matrix  $\underline{T}_v$  for the variational approximation is given by

$$\underline{T}_v = \frac{1}{N-iI'_{11}} \begin{bmatrix} (N-2)-iI'_{11} & -2\lambda_{11}P_{11} & -2\lambda_{21}P_{21} & \dots & -2\lambda_{s1}P_{s1} \\ -2P_{11}/\lambda_{11} & (N-2P_{11}^2)-iI'_{11} & -2P_{11}\lambda_{21}P_{21}/\lambda_{11} & \dots & -2P_{11}\lambda_{s1}P_{s1}/\lambda_{11} \\ -2P_{21}/\lambda_{21} & -2P_{21}P_{11}\lambda_{11}/\lambda_{21} & (N-2P_{21}^2)-iI'_{11} & \dots & -2P_{21}\lambda_{s1}P_{s1}/\lambda_{21} \\ \vdots & \vdots & \vdots & \ddots & \vdots \\ -2P_{s1}/\lambda_{s1} & -2P_{s1}P_{11}\lambda_{11}/\lambda_{s1} & \dots & \dots & (N-2P_{s1}^2)-iI'_{11} \end{bmatrix} \quad (10)$$

where  $N$  and  $P_{im}$  are the same as before (see Eqs.7 and 9) and

$$I'_{11} = k_1 \sum_j \frac{1}{k_j} \int_0^H \mu(n)\psi'(n, k'_j)\chi_1(n)dn \cdot \int_0^H \mu(z)\psi'(z, k'_j)\chi_1(z)dz \quad (11)$$

for the finite substratum problems (see Kazi (1979)) and

$$I'_{11} = \int_0^\infty \frac{dk'}{k'} \int_0^\infty \mu(n)\psi'(n, k')\chi_1(n)dn \cdot \int_0^\infty \mu(z)\phi'(z, k')\chi_1(z)dz \\ + i \int_0^\omega \frac{\omega}{\beta^2} \frac{dk'}{k'} \int_0^\infty \mu(n)\phi'(n, k')\chi_1(n)dn \cdot \int_0^\infty \mu(z)\phi'(z, k')\chi_1(z)kz \quad (12)$$

for the half-space problems (see Kazi (1978a)). If

$$\underline{A} = \begin{bmatrix} A_1 \\ A_1' \\ \vdots \\ A_s' \end{bmatrix} \quad \text{and} \quad \underline{B} = \begin{bmatrix} B_1 \\ B_1' \\ \vdots \\ B_s' \end{bmatrix} \quad \begin{matrix} (A'_s \text{ and } B'_s \text{ are the same} \\ \text{as in the expression for} \\ v(x, z) \text{ and } v'(x, z)) \end{matrix}$$

then the equations  $\underline{B} = \underline{T}_p \cdot \underline{A}$  and  $\underline{B} = \underline{T}_v \cdot \underline{A}$  yield the reflection and transmission co-efficients under both approximations.

#### PARTITIONING OF ENERGY

##### i) Finite Substratum Problems

The rate of energy flux across any vertical plane averaged over time is given by

$$\langle E \rangle = -\frac{1}{2} \text{Re} \int_0^H \frac{\partial v}{\partial x} \cdot \left( \frac{\partial v^*}{\partial t} \right) dz \quad (13)$$

where \* denotes the complex conjugate and Re denotes the real part.

(a) For an incident mode  $A_m e^{i(k_m x - \omega t)} \chi_m(z)$  from left to right in medium (I)

$$\begin{aligned} \langle E_m^i \rangle &= \frac{1}{2} \text{Re} \int_0^H \mu(z) k_m \omega A_m A_m^* \chi_m(z) \chi_m(z) dz \\ &= \frac{\omega}{2} k_m |A_m|^2 \int_0^H \mu(z) \chi_m(z) \chi_m(z) dz = \frac{\omega}{2} k_m |A_m|^2 \quad (m=1,2,\dots) \end{aligned} \quad (14)$$

because of normality of mode functions.

Similarly (b) for a reflected mode  $B_m e^{-i(k_m x + \omega t)} \chi_m(z)$  in medium I

$$\langle E_m^r \rangle = -\frac{\omega}{2} k_m |B_m|^2, \quad m = 1, 2, \dots, r. \quad (15)$$

(c) for an incident mode  $A'_m e^{-i(k'_m x + \omega t)} \chi'_m(z)$  in medium II:

$$\langle E_m'^i \rangle = -\frac{\omega}{2} k'_m |A'_m|^2, \quad m = 1, 2, \dots, s \quad (16)$$

and (d) for a reflected mode  $B'_m e^{i(k'_m x - \omega t)} \chi'_m(z)$  in medium II:

$$\langle E_m'^r \rangle = \frac{\omega}{2} k'_m |B'_m|^2, \quad m = 1, 2, \dots, s. \quad (17)$$

ia) Partitioning of Energy Under Plane Wave Approximation

Let  $\underline{A} = \begin{bmatrix} 0 \\ 1 \\ 0 \\ \vdots \\ 0 \end{bmatrix}$ . Then  $\underline{B} = \begin{bmatrix} B_1 \\ B_1' \\ B_2 \\ \vdots \\ B_s' \end{bmatrix} = \underline{T}_p \cdot \underline{A}$  is given by the second column of the

the matrix  $\underline{T}_p$  in equation (7); we get

$$\begin{bmatrix} B_1 \\ B_1' \\ B_2 \\ \vdots \\ B_s' \end{bmatrix} = \frac{1}{N} \begin{bmatrix} -2\lambda_{11} P_{11} \\ -2P_{11}^2 + N \\ -2P_{21} P_{11} \lambda_{11} / \lambda_{12} \\ \vdots \\ -2P_{s1} P_{11} \lambda_{11} / \lambda_{s1} \end{bmatrix} \quad (18)$$

Thus the transmission co-efficient is given by  $B_1 = -2\lambda_{11} P_{11} / N$  and the reflection coefficients are given by  $B_1' = -(2P_{11}^2 - N) / N$ ,  $B_2 = -(2P_{21} P_{11} \lambda_{11}) / \lambda_{21} N$ , ...  $B_s' = -(2P_{s1} P_{11} \lambda_{11}) / (\lambda_{s1} N)$ . The incident mode from right to left is supposed to be of unit amplitude. Using formulae in Eqs. (14) to (17), we obtain:

Total rate of incident energy flux averaged over time is

$$\langle E_1^i \rangle = -\frac{\omega}{2} k_1', \quad (19)$$

Total rate of transmitted energy flux averaged over time is

$$\langle E_1^T \rangle = \frac{-4\lambda_{11}^2 P_{11}^2 \omega k_1}{N^2} \cdot \frac{\omega k_1}{2} = \frac{-4P_{11}^2 \omega k_1'}{N^2} \cdot \frac{k_1'}{2} \quad (\because \lambda_{11} = \frac{k_1'}{k_1}) \quad (20)$$

Total rate of reflected energy flux averaged over time is

$$\begin{aligned} \langle E_1^r \rangle + \langle E_2^r \rangle + \dots + \langle E_s^r \rangle &= \frac{1}{N^2} \frac{\omega}{2} \{ (N - 2P_{11}^2)^2 k_1' + 4P_{21}^2 P_{11}^2 \left(\frac{\lambda_{11}}{\lambda_{21}}\right)^2 k_2' \\ &+ \dots + 4P_{s1}^2 P_{11}^2 \left(\frac{\lambda_{11}}{\lambda_{s1}}\right)^2 k_s' \} \end{aligned}$$

$$= \frac{1}{N^2} \frac{\omega k_1'}{2} \{ (1 + P_{21}^2 + \dots + P_{s_1}^2 - P_{11}^2)^2 + 4P_{21}^2 P_{11}^2 + \dots + 4P_{s_1}^2 P_{11}^2 \} \quad (21)$$

Hence the sum of the magnitudes of the transmitted and reflected energy flow rates averaged over time is

$$\begin{aligned} & \frac{1}{N^2} \frac{\omega k_1'}{2} \{ (1 + P_{11}^2 + \dots + P_{s_1}^2 - P_{11}^2)^2 + 4P_{11}^2 + 4P_{21}^2 P_{11}^2 + \dots + 4P_{s_1}^2 P_{11}^2 \} \\ &= \frac{1}{N^2} \frac{\omega k_1'}{2} (1 + P_{11}^2 + P_{21}^2 + \dots + P_{s_1}^2)^2 = \frac{\omega k_1'}{2} \end{aligned} \quad (22)$$

which is the total absolute value of the incident energy flow rate averaged over time. A similar argument leads to an energy balance equation for other incident modes.

ib) Partitioning of Energy Under Variational Approximation

$$\text{Let } \underline{A} = \begin{bmatrix} 1 \\ 0 \\ \vdots \\ 0 \end{bmatrix}, \text{ then } \underline{B} = \begin{bmatrix} B_1' \\ B_1' \\ \vdots \\ B_s' \end{bmatrix} = \underline{T}_v \cdot \underline{A} \text{ is given by the first column}$$

of Eq. (10). Thus the reflection co-efficient is  $B_1 = (N-2) - iI_{11}' / N - iI_{11}'$  and the transmission co-efficients are  $B_1' = -2P_{11} / \lambda_{11} (N - iI_{11}')$ ,  $B_2' = -2P_{21} / \lambda_{21} (N - iI_{11}')$  . . .  $B_s' = -2P_{s_1} / \lambda_{s_1} (N - iI_{11}')$ .

Proceeding as above and noting that  $I_{11}'$  is real, we have the sum of the magnitudes of total reflected and transmitted energy flux rates averaged over time:

$$\begin{aligned} \langle E_1'^t \rangle + \langle E_2'^t \rangle + \dots + \langle E_s'^t \rangle + \langle E_1'^r \rangle &= \frac{\omega k_1}{2(N^2 + I_{11}'^2)} \{ (N-2)^2 + 4P_{11}^2 \\ &+ 4P_{21}^2 + \dots + 4P_{s_1}^2 + I_{11}'^2 \} \\ &= \frac{\omega k_1}{2} = \langle E_1'^i \rangle, \quad \text{the total incident energy} \\ & \quad \text{flux averaged over time.} \end{aligned} \quad (23)$$

Since the total incident energy averaged over time is exactly partitioned into the time-average of the total reflected and total transmitted energies concentrated in normal modes, it follows that no energy is carried by the non-propagated modes in the finite substratum problems.

ii) Half-Space Problems

ia) Partitioning of Energy Under Plane Wave Approximation

Arguing as for the corresponding case in the finite substratum problems we can show that the sum of the magnitudes of the transmitted and reflected energy flow rates averaged over time equals the total absolute value of the incident energy flow rate averaged over time. However the situation is quite different under variational approximation.

iib) Partitioning of Energy Under Variational Approximation

For the half-space problems  $\text{Im}(I_{11}') > 0$  (see eq.(12)) and so the analysis for the corresponding case in the finite-substratum problems will show that

$$\begin{aligned} \langle E_1'^t \rangle + \langle E_2'^t \rangle + \dots + \langle E_s'^t \rangle + \langle E_1'^r \rangle &= \frac{\omega k_1}{2\{(N - \text{Re}I_{11}')^2 + \text{Im}(I_{11}')^2\}} \times \\ & \times \{(N-2 - \text{Re}I_{11}')^2 + (\text{Im}I_{11}')^2 + 4P_{11}^2 + 4P_{21}^2 + \dots + 4P_{s_1}^2\}, \\ \text{(with } N &= 1 + P_{11}^2 + \dots + P_{s_1}^2) \\ &= \frac{\omega k_1}{2} = \text{total incident energy.} \end{aligned}$$

Hence the total incident energy is greater than the sum of the energies reflected and transmitted in normal modes. Hence a part of incident energy escapes in the form of body waves and at certain frequencies the energy diffracted into body waves could be considerable (see Kazi (1978b), Niazy and Kazi (1980)).

#### DISCUSSION AND CONCLUSIONS

The problems associated with first two structures (Fig.1 & 2) are quite interesting from the point of view of the physics of Love wave propagation. While computing the dispersion curves for the phase velocity in the case of a strip overlying another strip, the dispersion effect disappears as the thickness of the layer with the higher shear wave velocity tends to zero. While this is expected, it shows that the simplistic interpretation of the dispersion effect as the result of constructive interference between internally reflected, plane SH waves in the horizontal direction within the layer (e.g. Grant & West, 1965) is not accurate, because decreasing the thickness of the high velocity layer does not change the reflection characteristics in the two layers.

The third and fourth structures (Fig. 3 & 4) are obviously quite significant in earthquake-engineering. For both cases the Love wave motion can not be represented in terms of normal modes only. The scattering of energy into body waves could be quite significant. It has been shown (Niazy & Kazi 1980) that in the case of the welded quarter spaces with a single layer (Fig.4) the body wave contribution can change the amplitude of the transmitted and reflected waves by almost an order of magnitude for certain frequencies when the velocity contrast is an order of magnitude on the two sides of the lateral discontinuity. For such large impedance contrast, the inclusion of the body wave contribution results in reflection and transmission coefficients that have many spike-like features. As an example, we consider the model given in Fig.5 and show transmission coefficients onto the soft medium in Figs 6(a,b). The spike-like features shown in Figs.6(a, b) are associated with the generation of the higher order Love modes in the softer medium. Although the contrast considered in this model appears to be an extreme limit, yet shear wave velocities less than 1 km/sec are not unusual in soft alluvium valleys next to solid rock mountains with shear wave velocities of the order of a few kilometers per second. As shown in Fig.6 (a,b) Love wave incident from the hard medium onto the soft medium may be magnified upon transmission by more than an order of magnitude for certain frequencies for the model shown in Fig.5. This magnification is a well-known phenomenon. However, the significance of the higher order modes in this high contrast case is rather surprising. Clearly, when designing an earthquake resistant building, the fundamental periods of the building should not coincide with the cut off periods for the Love modes of the medium below it, especially when the medium is a soft medium next to earthquake prone mountains.

#### ACKNOWLEDGEMENTS

The authors wish to thank the University of Petroleum and Minerals for providing excellent facilities and supporting our joint research project.

#### REFERENCES

- Grant, F.S. & West, G.F. 1965. Interpretation Theory in Applied Geophysics, McGraw Hill.
- Kazi, M.H., 1978a. The Love wave scattering matrix for a continental margin (theoretical) *Geophys. J.R. astr. soc.*, 52, 25-44.
- Kazi, M.H., 1978b. The Love wave scattering matrix for a continental margin (numerical), *Geophys. J.R. astr. soc.*, 53, 227-243.
- Kazi, M.H., 1979. Transmission, reflection and diffraction of Love waves in an infinite strip with a surface step, *J. Phys. A: Math. Gen.*, 12, 1441-1455.

Niazy, A. & Kazi, M.H., 1980a. On the Love wave scattering problem for welded layered quarter-spaces with application, submitted to Bull.Seis. soc. Am. for publication.

Niazy, A. & Kazi, M.H., 1980b. The Love wave scattering matrix for welded layered half-strip (of equal overall thickness) (under preparation).

Fig.5. Model showing material constants for the structure in Fig.4.

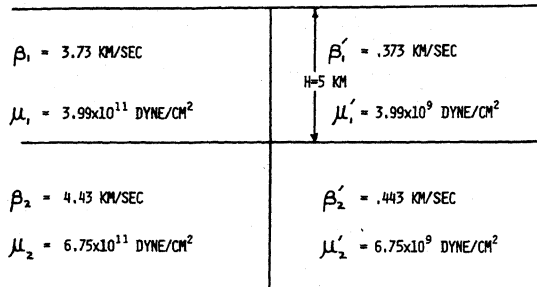


Fig.6(a). The absolute value of transmission co-efficients for a wave incident from left (hard) to right (soft) in the model given in Fig.5.

o: a sample point as a function of frequency, drawn at every other sample point (plane-wave approximation)

x: a sample point as a function of period, drawn at every other sample point (plane-wave approximation)

+: a sample point as a function of frequency, drawn at every other sample point (variational approximation)

\*: a sample point as a function of period, drawn at every other sample point (variational approximation)

(b). The same transmission co-efficients as in part (a) but plotted as functions of normalized wave number (kh) and normalized wave length ( $\lambda/h$ ).

